

Robust Secondary Voltage Control Scheme for Simultaneously Regulating Voltage Profile and Voltage Stability Using Synchrophasor

Heng-Yi Su ^{1*}, Feng-Ming Kang ¹, Yi-Chung Chen ²

¹ *Department of Electrical Engineering, Feng Chia University, Taichung, Taiwan, R.O.C*

² *Department of Information Engineering and Computer Science, Feng Chia University, Taichung, Taiwan, R.O.C*

*E-mail: hengyisu@fcu.edu.tw

Received : 10th August 2020

Revised on 28th September 2020;

Accepted: 03rd October 2020

Abstract—This paper proposes an robust control scheme based on synchronized phasor measurement unit (PMU) data for power system secondary voltage control. The proposed scheme utilizes both synchronized voltage magnitudes of monitored buses and the index of voltage stability margin as trigger signals to optimally control VAR sources in the improvement of voltage profile and enlargement of voltage stability margin in power systems. An extensive simulation studies on the IEEE 30-bus test system is carried out to demonstrate the feasibility and effectiveness of the proposed method.

Keywords— Automatic control, Phasor measurement unit (PMU), Power system control, Synchronized phasor (Synchrophasor), Secondary voltage regulation.

1. Introduction

Voltage instability has been regarded as one of the primary threats to security of power network operation during the last few years. In particular, several severe power system blackouts worldwide have been mainly attributed to voltage collapse problems [1]. The reason voltage instability and even voltage collapse take place is that the system cannot supply the demand, and the phenomenon is characterized by the losses of voltage control at certain locations in a power grid [2]-[3].

In order to provide a better voltage support in transmission networks, the coordinated voltage control has been developed. It is organized as a hierarchical structure with three levels: the primary, secondary, and tertiary voltage control. Significant attention has been given to the study of secondary level, which is an automatic regulation of voltage and reactive power for power systems. A lot of approaches for the design of secondary voltage controllers have been reported in the literature [4]-[16], some of which have been proven to be effective methods to guarantee the stability and security operation in some electric power industries of European countries [9]-[16]. The task of the secondary voltage control (SVC) is to mitigate the effect of voltage instability. The basic operation principle of the SVC can be summarized as follows: when voltage violations occur at certain key load buses which are designated as pilot nodes, the SVC will be enabled to keep the scheduled voltage profiles by optimal coordinated control of reactive power sources. However, just using voltage magnitudes at monitored buses alone may give an inaccurate indication of voltage stability in power systems [17]. This means that voltage stability issues cannot be fully prevented by the traditional SVC method. Therefore, an additional accepted measure of voltage stability is required for a more reliable SVC scheme.

The voltage stability margin, which is defined to be the distance from the power

system operating state to the voltage collapse, has been most widely used as the voltage stability indicator [18]-[26]. A variety of approaches based on different kinds of techniques has been proposed so far for voltage stability margin evaluation, such as sensitivity techniques [18]-[19], minimum singular value methods [20]-[21], and impedance-based index approaches [22]-[24]. Moreover, since load power margin is often associated with voltage stability margin, a number of papers uses load power margin as a monitoring index of voltage stability under a certain load level [25]-[26]. For example, the P-V curve is a useful tool for determining the load power margin information, and the complete P-V curve can be achieved by the continuation power flow (CPFLOW) method, which can deal with the divergence problem of the power flow analysis near the voltage collapse point [26].

In recent years, utilizing phasor measurement units (PMUs) to increase power grid situational awareness has become an active research area [27]-[28]. PMUs are precise power system measuring devices which have the capability of directly capturing time-synchronized measurements of the voltage phasors at the buses, as well as the current phasors on the incident lines. With increasing deployment of PMUs on transmission systems [29], synchrophasors are already available in wide-area. Indeed, these wide-area synchrophasors include enough information to analyze, predict, and control the voltage stability of a power system.

This paper is concerned with designing a new synchrophasor-based voltage stability enhancement scheme for safe power system operations. The rest of the paper is organized as follows: Section 2 describes the fundamental theories and mathematical principles of the proposed method. Numerical simulations and test results are given and discussed in section 3. Section 4 concludes the paper.

2. Operating Principles

The proposed scheme is able to achieve voltage stability enhancement tasks including power system voltage stability monitoring and control based on synchrophasor measurements. Fig. 1 illustrates the criteria for the activation of the proposed control strategy, in which the unshaded area represents the security operating region, while the shaded area represents the dangerous operating region. For example, if the power system is operated at the dangerous region; i.e. the system has poor voltage profile or insufficient VSM, then the proposed algorithm will be activated to steer the power system away from the critical point at which voltage collapses. The theory of the proposed method is discussed below.

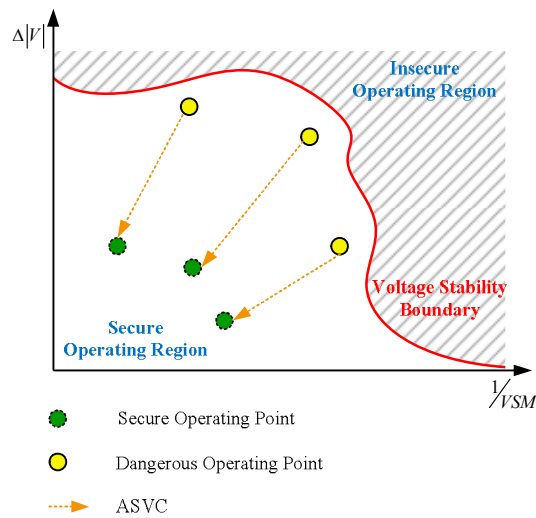


Fig. 1. Representation of the proposed control strategy.

2.1 Synchrophasor Technology

Synchrophasors are assumed to be provided from a PMU, which is known as a stand-alone physical device or a functional device within another device. Using the precise timing signal provided by global positioning system (GPS) as the common time base for PMUs, both the magnitude and the phase angle of the voltage and the current signals at different PMU locations can be measured, at exactly the same time instant in all

observable system buses. In addition, most of the PMUs available in the market follow the IEEE standard C37.118, which is currently the only standard worldwide for measuring power system synchrophasors. The standard defines synchrophasors, frequency, and rate of change of frequency (ROCOF) measurement under all operating conditions. A more detailed description about this standard can be referred to [30].

2.2 Voltage Stability Margin Estimation

A common voltage stability monitoring is expressed by the load power margin which shows how close the current operating point of a power system is to the point of collapse. In this study, we propose a method which employs the synchrophasor technique to speed up the continuation power flow (CPFLOW) tool to estimate the voltage stability margin in real-time. Detailed operations are presented as follows.

1) *Determination of Load Change Direction*: Load power margin estimations rely on load levels and load directions. However, distinct load changes can result in distinct voltage collapse points. This means that assessing the proximity of an operating point to voltage instability with consideration of load change direction is essential.

Suppose that there is a PMU installed at load bus i , which measures the voltage phasor V_i and the current phasor I_i . Utilizing two measurement pairs available from PMU, the complex load variation at bus i can be obtained by

$$\begin{aligned}\Delta S_i(k) &= S_i(k) - S_i(k-1) \\ &= V_i(k) \cdot I_i^*(k) - V_i(k-1) \cdot I_i^*(k-1)\end{aligned}\tag{1}$$

where the letter k represents the k th sampling point. It must be emphasized that the load change direction needs to be determined at the beginning of every run of the proposed margin computation.

2) *Thevenin Equivalent Network Method*: Next, we consider a load bus i connected to a complex power system, which can be simplified to a single-machine-infinite-bus

system by an estimated Thevenin equivalent network, as shown in Fig. 2. The rest of the power system is treated as its Thevenin equivalent voltage in series with Thevenin equivalent impedance.

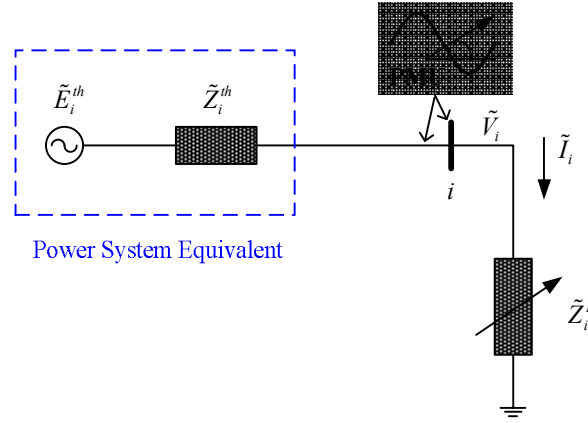


Fig. 2. Thevenin equivalent network at load bus i .

Application of Kirchoff's voltage law to this circuit results in

$$E_i^{th} = V_i + Z_i^{th} I_i \quad (2)$$

where E_i^{th} and Z_i^{th} correspond to Thevenin equivalent voltage and Thevenin equivalent impedance in phasor representation at bus i , respectively. Thus, using two sets of synchronized measured data, Thevenin equivalent parameters at the measuring point k can be solved as

$$E_i^{th}(k) = \frac{V_i(k-1)I_i(k) - V_i(k)I_i(k-1)}{I_i(k) - I_i(k-1)} \quad (3)$$

$$Z_i^{th}(k) = \frac{V_i(k-1) - V_i(k)}{I_i(k) - I_i(k-1)} \quad (4)$$

In addition, the load impedance of the complex load power S_i at the sampling point k is given by

$$Z_i^L(k) = \frac{|V_i(k)|^2}{S_i^*(k)} \quad (5)$$

Consequently, using PMU measurements, Thevenin equivalent network for a power system at a node can be acquired in real-time.

3) *Cubic Spline Extrapolation Method*: In Fig. 2, as voltage collapse occurs at bus i , the impedance-matching criterion holds; i.e. $|Z_i^{th}| = |Z_i^L|$. Moreover, $|Z_i^{th}|$ approximates to be a constant at increasing load levels. From this point of view, the estimated maximum loading point at which voltage collapses can be made by equating an approximating function, that extrapolates the trajectory of $|Z_i^L|$, to be $|Z_i^{th}|$.

In this research, the cubic spline extrapolation method is used as the function approximation. With cubic splines, approximate function is carried out by using third-order polynomials in the intervals between each successive pair of data points (the points are connected with curves). For example, given n data points, there are $n-1$ intervals, the mathematical formula of the polynomial in the j th interval, between points x_j and x_{j+1} is given by

$$f_j(x) = a_j x^3 + b_j x^2 + c_j x + d_j \quad (6)$$

for each $j = 1, 2, \dots, n-1$. Overall, there are $n-1$ equations, and since each cubic polynomial has four coefficients a_j , b_j , c_j , and d_j , the determination of all of the coefficients can be found by applying the method proposed in [31]. Notice that n is set to be three in this study; i.e. three sets of consecutive synchrophasors recorded at the PMU are utilized.

4) *Continuation Power Flow (CPFLOW) Method*: This approach provides a powerful tool to remain well-conditioned at and around the voltage collapse point of P-V curves in power flow calculation based on a locally parameterized continuation technique [26]. However, the conventional CPFLOW tool faces the difficulties associated with the lack of the input and guidance of real-time measurement information; thereby, the results are

usually inaccurate, and even the computational procedure is too slow to satisfy real-time operational requirements.

In this research, we develop a hybrid method for fast as well as accurate voltage stability margin computation by combing both measurement-based and CPFLOW based techniques. To illustrate this, suppose that a load is increased by altering the load parameter λ up to the critical load or the maximum loading point λ^{\max} . The proposed method includes two stages in computational operations.

Stage 1) Measurement-based technique: Compute the estimated maximum loading point, denoted by λ^{es} , by using an estimated Thevenin equivalent network approach with cubic spline extrapolation technique. Meanwhile, load change direction toward the maximum loading point is determined by two consecutive sets of PMU measurements.

Stage 2) CPFLOW based technique: Initiate a CPFLWO algorithm to find the actual maximum loading point, λ^{\max} , according to the estimated point at λ^{es} as well as the measured direction of load change. Afterward, the load power margin is calculated as $\lambda^{\max} - \lambda^0$, in which λ^0 is the base case loading point.

Using the approach above, the VSM, which is defined by the percentage of the load power margin, can be computed as

$$VSM = \frac{\lambda^{\max} - \lambda^0}{\lambda^0} \times 100\% \quad (7)$$

2.3 Robust Automatic Voltage Control

Consider the linearized model of decoupled power flow equations, as follows:

$$[\Delta \mathbf{Q}] = B[\Delta \mathbf{V}] \quad (8)$$

where B is the system susceptance matrix, $\Delta\mathbf{Q}$ and $\Delta\mathbf{V}$ stand for the reactive power change and voltage magnitude change vectors, respectively. To formulate the steady-state voltage-var control, (8) can be written as

$$\begin{bmatrix} \Delta\mathbf{Q}_G \\ \Delta\mathbf{Q}_L \end{bmatrix} = \begin{bmatrix} B_{GG} & B_{GL} \\ B_{LG} & B_{LL} \end{bmatrix} \begin{bmatrix} \Delta\mathbf{V}_G \\ \Delta\mathbf{V}_L \end{bmatrix} \quad (9)$$

where the subscripts L and G are used to represent the load buses (P-Q buses) and the voltage-controlled buses (P-V buses), respectively. In the above matrix equation, let

$$\begin{aligned} \mathbf{q} &= \Delta\mathbf{Q}_L \\ \mathbf{u} &= \Delta\mathbf{Q}_G \end{aligned} \quad (10)$$

be the notations of reactive power load disturbances and control decisions to participating controllers, respectively. Then, load voltage deviations $\Delta\mathbf{V}_L$ can be expressed in terms of \mathbf{q} and \mathbf{u} as

$$\Delta\mathbf{V}_L = J_1\mathbf{q} - J_2\mathbf{u} \quad (11)$$

where

$$\begin{aligned} J_1 &= (B_{LL} - B_{LG}B_{GG}^{-1}B_{GL})^{-1} \\ J_2 &= J_1(B_{LG}B_{GG}^{-1}) \end{aligned} \quad (12)$$

Notice that J_1 and J_2 are the matrices relating to system configurations. In this case, the first term in (11) denotes uncontrolled load voltage variations in response to load disturbances \mathbf{q} , while the second term denotes the effect of control outputs \mathbf{u} on voltage changes at load buses.

In secondary voltage controller design, a linear feedback control structure is applied. It uses voltage magnitudes at monitored buses as inputs, and generates control actions as outputs. Furthermore, it must be stressed that only the voltage information at the pilot buses are available to the control devices. If there are sufficient measurement units at all load buses, voltage changes $J_1\mathbf{q}$ will be the control inputs. In practical applications,

however, only portions of load buses are acting as pilot buses. That is, the voltage deviations at these monitored buses is expressed as

$$\Delta \mathbf{V}_p = J_p \mathbf{q} \quad (13)$$

where J_p is the rows of J_1 corresponding to the selected pilot points. Indeed (In fact), $\Delta \mathbf{V}_p$ are only some entries of the vector $J_1 \mathbf{q}$. In this case, linear control vector \mathbf{u} is given by

$$\mathbf{u} = K \Delta \mathbf{V}_p = K (J_p \mathbf{q}) \quad (14)$$

where K denotes the control gain matrix that needs to be determined. Replacing the second term of (11) with the control outputs \mathbf{u} in (14) results in

$$\begin{aligned} \Delta \mathbf{V}_L &= J_1 \mathbf{q} - J_2 K \Delta \mathbf{V}_p \\ \text{or} \\ \Delta \mathbf{V}_L &= (J_1 - J_2 K J_p) \mathbf{q} \end{aligned} \quad (15)$$

Suppose that system load disturbances \mathbf{q} are within a certain limit γ in a practical power system; i.e.

$$\|\mathbf{q}\|_\infty \leq \gamma \quad (16)$$

Under this assumption, the optimal robust gain matrix K^* such that the worst-case load voltage change is minimized is given by

$$\min_{K^*} \max_{\|\mathbf{q}\|_\infty \leq \gamma} \|(J_1 - J_1 K^* J_p) \mathbf{q}\|_\infty \quad (17)$$

The minimization problem in (17) is also equivalent to

$$\min_{K^*} \|J_1 - J_2 K^* J_p\|_\infty \quad (18)$$

From the preceding equation, one can see that the optimal robust gain matrix K^* depends entirely on system configurations on pilot-point locations. In other words, K^* remains the same regardless of any unexpected load disturbance. The optimization

problem in (18) can be reformulated as an linear program [32], and solved by using a linear programming solver such as *linprog* function in the MATLAB optimization toolbox [33].

3. Simulation Results

This section presents numerical examples of the proposed scheme, i.e. enhancement of voltage stability, on a sample power system. The IEEE 30-bus system is used as an example to show the effectiveness of the proposed method. This sample system consists of 41 transmission lines, 6 generators, and 24 loads. The system data including line parameters and bus data are given in [34]. The simulation program is coded using MATLAB and implemented on a PC which has a CPU with Intel® Core™2 Duo 2.66 GHz and a memory with 4 GB.

The pilot-bus locations, in which PMUs are to be installed, are selected from those 24 load buses. The threshold levels for triggering the proposed control algorithm are defined as follows: when the power system operates at the dangerous region, i.e. the measured voltage of the i th PMU is less than 0.9 p.u. or the computed value of the voltage stability margin is less than 10%. The voltage profile improvement index used in this research is expressed by the root mean square value of voltage changes at all load buses

$$x^{rms} = \left(\frac{1}{m} \sum_{j=1}^m \|x_j\|_2^2 \right)^{1/2} \quad (19)$$

where m is the number of load buses in the test system, and x_j for each $j = 1, 2, \dots, m$ denotes the resulting voltage change at each of the load buses. In this test system, m is set to be 24.

In order to investigate the robustness of the proposed method, comprehensive experiments with respect to different load levels, different load patterns, various branch

outage contingencies, and various pilot-bus selections have been studied. Due to the space limited, in this work, only the results under the scenario depicted in Fig. 3 are presented. The VAR sources and the PMU locations considered in this test condition are listed below:

- VAR sources: Bus 1, 2, 5, 8, 11, 13
- PMU locations: Bus 17, 23

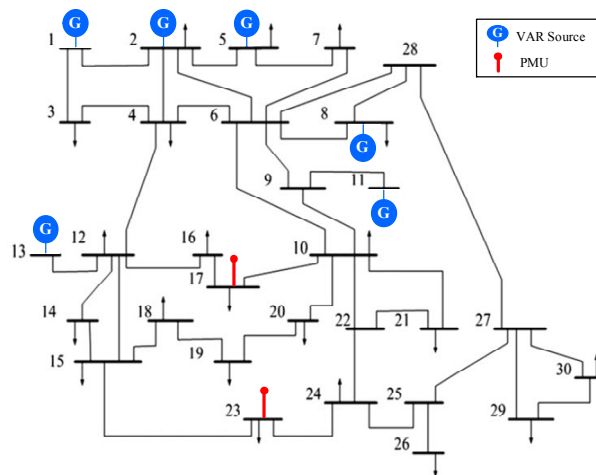


Fig. 3. One-line diagram of the IEEE 30-bus test system with PMUs.

The simulation results for the selected cases shown in Fig. 4 are briefly summarized in the following.

IEEE 30-bus Test System:

- VAR Sources: Bus 1, 2, 5, 8, 11, 13
- PMUs: Bus 17, 23
- Three Cases:

Case	System / Bus Load Change Pattern	Light / Peak Load Condition	With / Without Line Outage Contingency
I	System	Light	Without
II	Bus	Peak	Without
III	System	Peak	With

↓

Fig. 4. Simulation scenarios for the cases presented in this paper.

3.1 Case I

In the first test case, system load change pattern is simulated: all the loads in the IEEE 30-bus system are increased simultaneously based on their initial load levels. The test system is operating at a light load condition, in which the voltage magnitudes obtained from the PMUs are $V_{17} = 0.9333$ p.u. and $V_{23} = 0.8837$ p.u., while the value of VSM calculated by the proposed voltage stability margin estimation method is $VSM = 28.03\%$.

In this case, low voltage violation occurs at bus 23 since $V_{23} = 0.8837$ p.u. is less than the pre-determined value of 0.9 p.u.. This will activate the proposed method, and the effect of the control strategy is shown in Fig. 5. From the shown figure, one can see that the voltage magnitude of bus 23 is improved from 0.8837 to 0.9579 p.u.. Also, the maximum load power is increased from 423 to 478 MW.

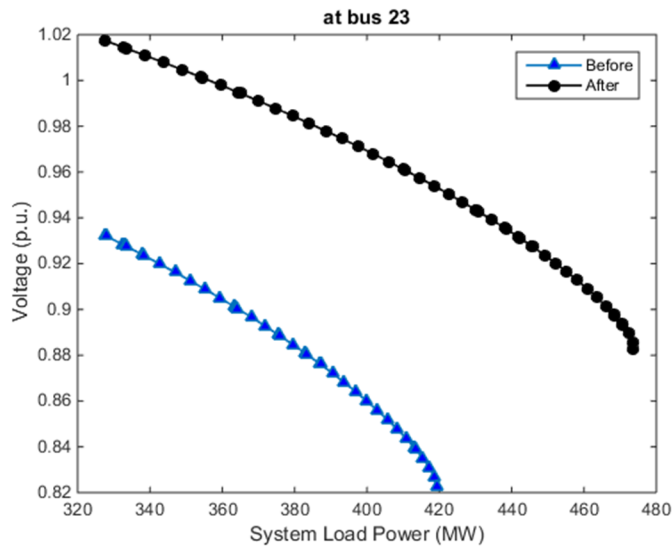


Fig. 5. Case I: Enhancement of voltage stability using the proposed method on the IEEE 30-bus test system: V_{23} is improved from 0.8837 to 0.9579 p.u., and the maximum load power is increased from 423 to 478 MW.

3.2 Case II

In this case, bus load change pattern is considered. Only the load at bus 30 is increased proportionally to its initial load level. The test system is investigated under peak load conditions and is operated in the dangerous region. The measured voltages and the computed VSM without control actions are $V_{17} = 0.9248$ p.u., $V_{23} = 0.9472$ p.u., and $VSM = 9.47\%$, respectively.

Although voltage magnitudes at the monitored buses are at acceptable voltage levels, voltage stability margin of the entire power system is insufficient. Under such a situation, no control actions will be taken by the use of the traditional SVC methods, which means that the system has high risk of voltage collapse. In contrast, voltage instability, leading to voltage collapse, will be detected by the proposed scheme because of $VSM = 9.47 < 10\%$, so that the proposed method will be triggered for improving the overall system voltage stability.

The simulation result is illustrated in Fig. 6, showing that the maximum load power is significantly increased from 403 to 475 MW, as well as V_{17} improved from 0.9248 to 1.0076 p.u..

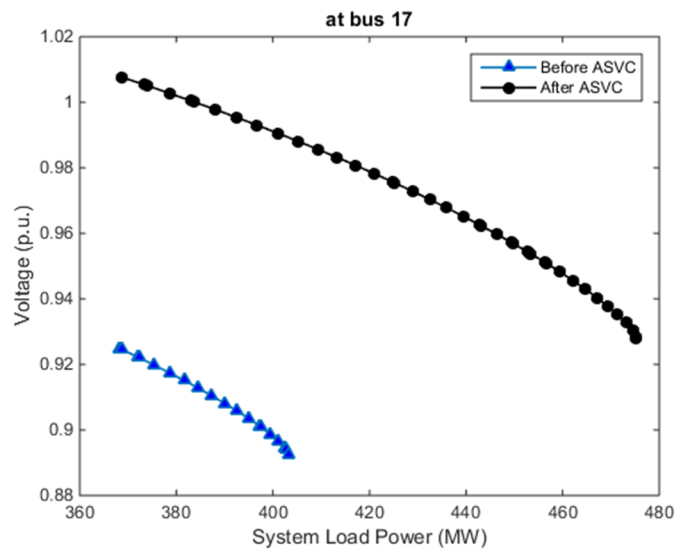


Fig. 6. Case II: Enhancement of voltage stability using the proposed method on the IEEE 30-bus test

system: V_{17} is improved from 0.9248 to 1.0076 p.u., and the maximum load power is increased from 403 to 475 MW.

3.3 Case III

In the third simulation, the load change pattern is the same as in Case I. The test system is investigated under stressed conditions, and the line #10-20 is studied under branch outage contingency condition. The system is operating in the dangerous region, which could result $V_{17} = 0.8773$ p.u. and $V_{23} = 0.8786$ p.u. before control actions performed. At this operating point, the estimated value of the voltage stability margin is $VSM = 8.39\%$. Since the system has poor voltage level and inadequate VSM, voltage instability is determined. Accordingly, the proposed method will be activated to prevent imminent voltage collapse. Fig. 7 shows the simulation result. In Fig. 7, it is clearly seen that the voltage stability of the system is considerably enhanced after the proposed method.

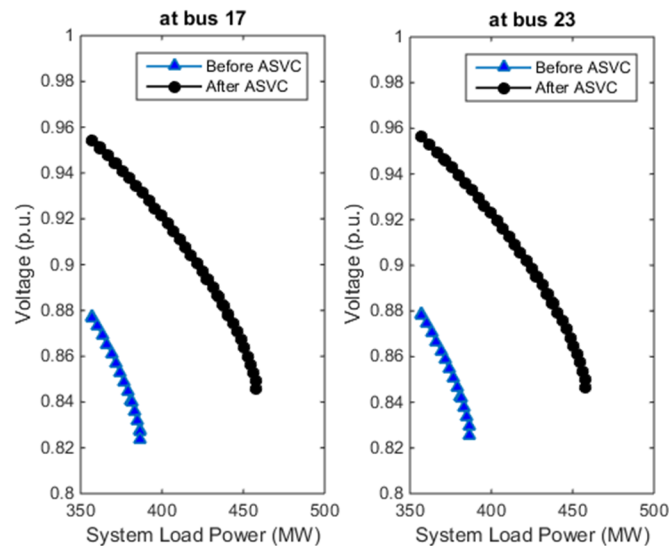


Fig. 7. Case III: Enhancement of voltage stability using the proposed method on the IEEE 30-bus test system. (a) V_{17} is improved from 0.8773 to 0.9544 p.u., and the maximum load power is increased from 387 to 458 MW. (b) V_{23} is improved from 0.8786 to 0.9566 p.u., and the maximum load power is

increased from 387 to 458 MW.

Table I summarizes the test results for the above three cases. An inspection from the shown table indicates that the performance of the power system is greatly improved. This means that the control decisions provided by the proposed scheme is efficient and effective for the enhancement of the overall power system voltage stability.

TABLE I

Performance Evaluation for the Proposed Scheme to the Enhancement of Voltage Stability on the IEEE 30-bus Test System

Case	Voltage Profile Improvement Index x^{ms} (p.u.)		Voltage Stability Margin VSM (%)	
	Before	After	Before	After
I	0.06438	0.03819	28.03	44.55
II	0.10398	0.06146	9.47	28.86
III	0.12023	0.07133	8.39	28.14

4. Conclusion

In order to achieve secure and reliable grid operations, a method, which employs the synchrophasor technique for power system voltage stability monitoring and control, is presented. With this new approach, the overall network voltage can be improved, as well as system voltage stability by an appropriate reactive power management against voltage instability. The proposed scheme has been applied to the IEEE 30-bus test system, and successful results have been obtained.

Acknowledgements

This work was supported in part by the Ministry of Science and Technology of Taiwan, R.O.C., under Contracts MOST 103-2221-E-035-101 and MOST 103-2218-E-035-018.

References

- [1] C. W. Taylor, *Power System Voltage Stability*. New York: McGraw-Hill, 1994.
- [2] T. Van Cutsem and C. Vournas, *Voltage Stability of Electric Power Systems*. Norwell, MA: Kluwer, 1998.
- [3] P. Kundur, *Power System Stability and Control*. New York: McGraw-Hill, 1994.
- [4] J. S. Thorp, M. Ilic-Spong, and M. Varghese, "An optimal secondary voltage-var control technique," *Automatica*, vol. 22, no. 2, pp. 217–222, 1986.
- [5] M. Ilic, J. Christensen, and K. L. Eichorn, "Secondary Voltage Control using Pilot Point Information," *IEEE Trans. Power Syst.*, vol. 3, no. 2, pp. 660–668, May 1988.
- [6] A. Stankovic, M. Ilic, and D. Maratukulam, "Recent results in secondary voltage control of power systems," *IEEE Trans. Power Syst.*, vol. 6, no. 1, pp. 94–101, Feb. 1991.
- [7] A. Zobjan and M. D. Ilic, "A steady state voltage monitoring and control algorithm using localized least square minimization of load voltage deviations," *IEEE Trans. Power Syst.*, vol. 11, no. 2, pp. 929–938, May 1996.
- [8] H. Wang, H. Li, and H. Chen, "Coordinated secondary voltage control to eliminate voltage violations in power system contingencies," *IEEE Trans. Power Syst.*, vol. 18, no. 2, pp. 588–595, May 2003.
- [9] J. P. Paul, J. T. Leost, and J. M. Tesson, "Survey of the secondary voltage control in France: Present realization and investigations," *IEEE Trans. Power Syst.*, vol. PWRS-2, no. 2, pp. 505–511, May 1987.
- [10] P. Lagonotte, J. C. Sabonnadiere, J. Y. Leost, and J. P. Paul, "Structural analysis of the electrical system: Application to the secondary voltage control in France," *IEEE Trans. Power Syst.*, vol. 4, no. 2, pp. 1477–1484, May 1989.
- [11] S. Corsi, P. Marannino, N. Losignore, G. Moreschini, and G. Piccini, "Coordination between the reactive power scheduling function and the hierarchical voltage control of the EHV ENEL system," *IEEE Trans. Power Syst.*, vol. 10, no. 2, pp. 686–694, May 1995.
- [12] H. Vu, P. Pruvot, C. Launay, and Y. Harmand, "An improved voltage control on large scale power system," *IEEE Trans. Power Syst.*, vol. 11, no. 3, pp. 1295–1303, Aug. 1996.
- [13] J. L. Sancha, J. L. Fernandez, A. Cortes, and J. T. Abarca, "Secondary voltage control: Analysis, solutions, simulation results for the Spanish transmission system," *IEEE Trans. Power Syst.*, vol. 11, no. 2, pp. 630–638, May 1996.
- [14] S. Corsi, M. Pozzi, C. Sabelli, and A. Serrani, "The coordinated automatic voltage control of the Italian transmission grid-Part I: Reasons of the Choice and Overview of the Consolidated Hierarchical System," *IEEE Trans. Power Syst.*, vol. 19, no. 4, pp. 1723–1732, Nov. 2004.
- [15] S. Corsi, M. Pozzi, M. Sforza, and G. Dell'Olio, "The coordinated automatic voltage control of the Italian transmission grid-part II: control apparatuses and field performance of the consolidated hierarchical system," *IEEE Trans. Power Syst.*, vol. 19, no. 4, pp. 1733–1741, Nov. 2004.
- [16] C. Yu, Y. T. Yoon, M. D. Ilic, and A. Catelli, "On-line voltage regulation: The case of New England," *IEEE Trans. Power Syst.*, vol. 14, no. 4, pp. 1477–1484, Nov. 1999.
- [17] M. Begovic et al., "Summary of system protection and voltage stability," *IEEE Trans. Power Del.*, vol. 10, no. 2, pp. 631–638, Apr. 1995.
- [18] N. Flatabo, R. Ognedal, and T. Carlsen, "Voltage stability condition in a power transmission system calculated by sensitivity methods," *IEEE Trans. Power Syst.*, vol. 5, no. 4, pp. 1286–1293, Nov. 1990.
- [19] N. Flatabo, O. Fosso, R. Ognedal, and T. Carlsen, "A method for calculation of margins to voltage instability applied on the Norwegian system for maintaining required security level," *IEEE Trans. Power Syst.*, vol. 8, no. 3, pp. 920–928, Aug. 1993.
- [20] P. A. Lof, T. Semed, G. Andersson, and D. J. Hill, "Fast calculation of a voltage stability index," *IEEE Trans. Power Syst.*, vol. 7, no. 1, pp. 54–64, Feb. 1992.
- [21] P. A. Lof, G. Andersson, and D. J. Hill, "Voltage stability indices for stressed power systems," *IEEE Trans. Power Syst.*, vol. 8, no. 1, pp. 326–335, Feb. 1993.
- [22] K. Vu, M. M. Begovic, D. Novosel, and M. M. Saha, "Use of local measurements to estimate voltage-stability margin," *IEEE Trans. Power Syst.*, vol. 14, no. 3, pp. 1029–1035, Aug. 1999.
- [23] I. Smon, G. Verbic, and F. Gubina, "Local voltage-stability index using Tllegen's theorem," *IEEE Trans. Power Syst.*, vol. 21, no. 3, pp. 1267–1275, Aug. 2006.
- [24] S. Corsi, G. N. Taranto, "A real-time voltage instability identification algorithm based on local phasor measurements," *IEEE Trans. Power Syst.*, vol. 23, no. 3, pp. 1271–1279, Aug. 2008.
- [25] H. D. Chiang, A. J. Flueck, K. S. Shah, and N. Balu, "CPFLOW: A practical tool for tracing power system steady-state stationary behavior due to load and generation variations," *IEEE Trans. Power Syst.*, vol. 10, no. 2, pp. 623–634, May 1995.
- [26] V. Ajarapu and C. Christy, "The continuation power flow: A tool for steady state voltage stability analysis," *IEEE Trans. Power Syst.*, vol. 7, no. 1, pp. 416–423, Feb. 1992.

- [27] A. G. Phadke and J. S. Thorp, *Synchronized Phasor Measurements and Their Applications*. New York: Springer-Verlag, 2008.
- [28] J. De La Ree, V. Centeno, J. S. Thorp, and A. G. Phadke, "Synchronized phasor measurement applications in power systems," *IEEE Trans. Smart Grid*, vol. 1, no. 1, pp. 20–27, Jun. 2010.
- [29] N. M. Manousakis, G. N. Korres, and P. S. Georgilakis, "Taxonomy of PMU Placement Methodologies," *IEEE Trans. Power Syst.*, vol. 27, no. 2, pp. 1070–1077, May 2012.
- [30] K. E. Martin, "Synchrophasor standards development-IEEE C37.118 & IEC 61850," *Proceedings of the 44th Hawaii International Conference on System Sciences*, 2011.
- [31] C. de Boor, *A Practical Guide to Splines*. New York: Springer-Verlag, 1978.
- [32] S. Boyd and L. Vandenberghe, *Convex Optimization*. Cambridge University Press, 2004.
- [33] MathWorks, Inc., *MATLAB optimization toolbox*. [Online]. Available: <http://www.ee.washington.edu/re-serach/pstcal/>.
- [34] *Power Systems Test Case Archive*, University of Washington College of Engineering. [Online]. Available: <http://www.ee.washington.edu/re-serach/pstcal/>.